Nuclear Instruments and Methods in Physics Research B 542 (2023) 7–13

Contents lists available at ScienceDirect

Nuclear Inst. and Methods in Physics Research, B

journal homepage: www.elsevier.com/locate/nimb

Enhanced surface quality and properties of cold spray Al coating by high current pulsed electron beam treatment

Wei Jiang [*], Yuanliang Sun, Hongbin Dai, Enhao Wang

School of Materials Science and Chemical Engineering, Harbin University of Science and Technology, Harbin, China

A R T I C L E I N F O

Keywords:
High current pulsed electron beam
Aluminum coating
Wear resistance
Corrosion resistance
Electrochemical impedance spectroscopy

A B S T R A C T

In this paper, high current pulsed electron beam (HCPEB) irradiation was employed to improve the surface density and properties of cold spray Al coating. The effects of the energy density on the microstructure, phase composition, stress, microhardness, wear, and corrosion behavior of coatings as-fabricated were investigated. HCPEB remelting treatment has improved the surface defects of cold spray coatings. The microhardness of treated coatings is higher than that of untreated coating, and the highest microhardness of the treated coatings occurs in the subsurface layer of the coatings. The wear track width and depth of the treated coating were lower than those of the untreated sample. The corrosion potential of the treated samples increases from −1.12 v to −0.95 v, and the corrosion current density reduces from 15.64 μA/cm^2 to 3.31 μA/cm^2. Our results demonstrated the wear and corrosion resistance of the cold spraying Al coating were dramatically improved by HCPEB irradiation.

1. Introduction

Aluminum, titanium, and magnesium and their alloys are ideal choices for light metallic structural material because of their low density and high specific properties [1]. Magnesium and its alloys are of great significance for lightweight design and manufacturing in the fields of aviation, biomedicine, automobile, and electronics [2,3]. However, the chemical properties of magnesium are very active. The standard electrode potential is −2.36 V and poor corrosion resistance restricts the application of magnesium and magnesium alloys [4]. Because of the low hardness, the wear resistance of the magnesium surface is also low. Therefore, the surface protection of magnesium alloys has become a research hotspot for its further promotion and application.

At present, many surface techniques and composition modifications are employed to lengthen the service life of magnesium and its alloys, which include alloying [5], ion implantation [6], spray [7], electroplating [8], physical vapor deposition films [9], high energy beam surface modification [10,11], micro-arc oxidation [12], chemical conversion treatment [13], etc. These methods have addressed the corrosion and wear problems of magnesium and magnesium alloys in varying degrees, promoting the wider applications of magnesium and magnesium alloys.

As one of the most effective methods, the coating technique is used to improve the performance of magnesium and its alloys in harsh conditions. Cold spray is a process where the solid particles are heated at low temperatures and the particles can be accelerated up to 1200 m/s [14]. Plastic deformation of the substrate can occur due to the enormous energy caused by the particle impact. Different from traditional thermal spraying, the high kinetic energy and low thermal energy achieved during cold spraying can reduce residual stresses, the porosity of coating, oxidation, and degradation of the feedstock material [15–17]. Therefore, for substrates or spray materials that are sensitive to heat or oxidation, cold spray can be used as a promising process for synthesizing protective coatings [18,19]. Previous studies have reported the possibility of protecting magnesium and magnesium alloys using aluminum and its alloy cold spray coatings [20,21]. High current pulsed electron beam (HCPEB) is a kind of surface modification method that appeared in recent decades. In most cases, HCPEB irradiation is accompanied by surface remelting, which will improve surface properties and effectively restrain the porosity of coating material [22–25].

In this study, the Al coating was prepared by cold spray method on AM50 magnesium alloy substrate and HCPEB irradiation treatment. The effects of HCPEB energy density on the surface microstructure evolution, phases, and the wear resistance and corrosion resistance of the coatings were studied.

* Corresponding author.
E-mail address: jiangwei@hrbust.edu.cn (W. Jiang).

https://doi.org/10.1016/j.nimb.2023.06.002
Received 10 April 2023; Received in revised form 16 May 2023; Accepted 2 June 2023
Available online 10 June 2023
0168-583X/

2. Experimental

2.1. Coating preparation

The Al powders (granularity 300 mesh) were deposited on the AM50 substrate ($\Phi = 20$ mm and $h = 4$ mm) using cold spray equipment created. The chemical composition of the AM50 substrate is presented in Table 1. Before cold spray deposition, the substrate was sandblasted using SiO_2 grit. The cold spray system used compressed air as the accelerating gas and carrier gas for powder feeding. During the cold spray deposition process, the gas pressure was fixed at 0.8 MPa. The gas temperature was kept no more than 200 ℃.

2.2. Electron beam irradiation

Samples were irradiated in argon at a pressure of 6.0×10^{-2} Pa. Both 3 and 4.5 J/cm^2 are the HCPEB energy densities. The cathode was 100 mm away from the substrate, and there were 30 pulses in total. The HCPEB irradiation samples were covered elsewhere [26].

2.3. Structural and morphological, characterization

In order to evaluate the surface and cross-section morphology of the samples, a scanning electron microscope (SEM, Helios Nanolab 600i) and an optical microscope (KEYENCE, VHX-1000E) were utilized. Additionally, the structural and phase analysis of the samples was conducted using the X-ray diffraction technique. Residual stress on the surface of samples was measured by X-ray diffraction stress analyzer before and after HCPEB treatment. Microhardness testing was conducted on the cross sections of the samples using a Vickers hardness tester with a load of 0.025 kg and a holding time of 15 s. To ensure the repeatability of the microhardness characterization, the average of five values was conducted on each test position. A CJS111A rotational friction and wear tester was used to conduct a friction and wear test. The test parameters included a friction pair of Si_3N_4 ceramic balls with a diameter of 5 mm, a normal load of 30 N, a rotational speed of 350 r/min, a friction radius of 2 mm, and a duration of 360 s. Corrosion tests were performed on samples with and without HCPEB irradiation treatment using electrochemical polarization technology. The corrosion tests of the coatings were evaluated using a conventional three-electrode cell. The coating was used as the working electrode, while a platinum wire electrode and saturated calomel electrode were used as the counter and reference electrodes, respectively. The sample area exposed to the NaCl water solution was 1 cm^2 and the tests were conducted at room temperature. Before the measurement, all samples were soaked in 3.5 wt% NaCl water solution for 30 min to make sure that the open circuit potential was stable for all tests. The corrosion current (I_{corr}) and corrosion potential (E_{corr}) were calculated from Tafel curves with a scan rate of 0.33 mV/s.

3. Results and discussion

As shown in Fig. 1, the surface morphology of the untreated sample and the ones subjected to HCPEB irradiation at respective energy densities of 3 and 4.5 J/cm^2 for 30 pulses. Fig. 1a shows the surface morphology of the untreated cold sprayed coating sample, which has the typical feature of cold sprayed coating. The surface was highly rough and undulating. During the cold spray process, coating materials were retained in the solid and were deposited on the surface of the substrate with a high-velocity impact and severe plastic deformation. Fig. 1b and Fig. 1c show the surface morphology of HCPEB treated Al coating. The energy was deposited on the material surface during HCPEB treatment, which leads to the process of heating, melting, and solidification on the material surface. It can be seen that the rough surface of cold spraying coatings was remelted, and the coating surface became more smooth and dense. With the increase of irradiation energy density, as shown in Fig. 1c, the non-molten particles began to melt and merge to form the larger and connected remelted zone.

Fig. 2 shows the cross-section morphology of untreated and HCPEB treated samples. The HCPEB irradiation leads to the surface melting of cold spraying Al coating. When the energy density is 3 J/cm^2, the coating was remelted after HCPEB treated, and the average thickness of the remelted layer is about 15 μm (Fig. 2b). With the energy density increasing to 4.5 J/cm^2, the surface melting was intensified, and the average thickness of the remelted layer increased to about 20 μm (Fig. 2c).

Fig. 3 shows the three-dimensional surface morphology of HCPEB treated Al coatings. It can be seen that there are protrusions and valleys on the surface of the untreated coating sample. With the increasing energy density of HCPEB irradiation, the remelting of non-molten particles was intensified, and the discrete remelted zone can be merged. The more smooth and dense surface with smaller cavities and protrusions proved that the mechanical and corrosion resistance improved after HCPEB treatment. The gradient coating can evidently enhance the structural stability after the intermediate transition layer Al is used, which can make the surface denser [27].

Fig. 4 gives the phase composition change of cold spray Al coating after HCPEB treatment. For the untreated sample, the diffraction peaks coincided well with the aluminum phase composition and the corundum phase composition. After the HCPEB irradiation with energy densities 3 and 4.5 J/cm^2, the diffraction peaks of aluminum and corundum phase composition still were observed in treated coatings, and no new phase was created in coatings after the HCPEB irradiation.

The results of the residual stress measurement are shown in Fig. 5. The compressive residual stress of the untreated Al coating is about −19 MPa. After HCPEB treatment, compressive residual stress of –23 MPa occurs at an irradiation energy density of 3 J/cm^2 and then reduces to −31 MPa at an irradiation energy density of 4.5 J/cm^2. The variation tendency of residual stress is attributed to the following reasons. For the untreated cold spray coating sample, the particles impact the substrate at high velocity in the solid state, and residual stress is usually compressive [28]. For the two HCPEB treated coating samples, remelting occurred on the coating top, along with the volume change, but the bottom coating was unmelted and produced a restrain to the top remelted coating, leading to the formation of compressive residual stress. Consequently, the compressive residual stress of the coating surface was increased after HCPEB irradiation.

Fig. 6 shows the changes in microhardness of cold spray Al coating before and after HCPEB treatment. The microhardness of the untreated coating is around 56 HV. After the HCPEB treatment, the surface microhardness of the coating is increased to approximately 69 and 63 HV with the irradiation energy density of 3 and 4.5 J/cm^2, respectively. The microhardness of the treated coatings first increases and then decreases with the increase of depth, and finally converges with that of the untreated coatings. The highest microhardness of the treated coatings occurs in the subsurface layer of the coatings, which is 73 and 85 HV, respectively. The location where the highest value of hardness appears becomes deeper with increasing irradiation energy density. The enhancement of the microhardness is mainly attributed to surface densification and dynamic strain hardening induced by HCPEB irradiation. The changing trend of microhardness is in agreement with the previous publication [29–32].

Fig. 7 plots the friction coefficient under a load of 30 N for HCPEB treated and untreated coating samples. The friction coefficients of the untreated sample have a large range change during the whole testing, while the friction coefficients in the treated samples are relatively stable.

Table 1
Chemical composition of AM50 magnesium alloy.

Composition	Al	Zn	Mn	Si	Mg
Percent(wt,%)	4.5 ~ 5.3	≤0.02	0.28 ~ 0.5	≤0.50	balance

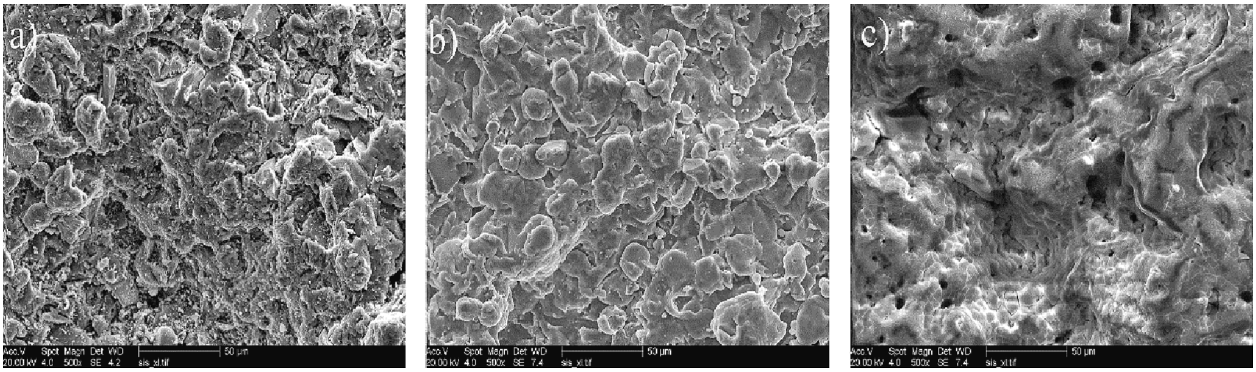

Fig. 1. Surface morphology of the coating after irradiation with different energy density a) untreated; b) 3 J/cm^2; c) 4.5 J/cm^2.

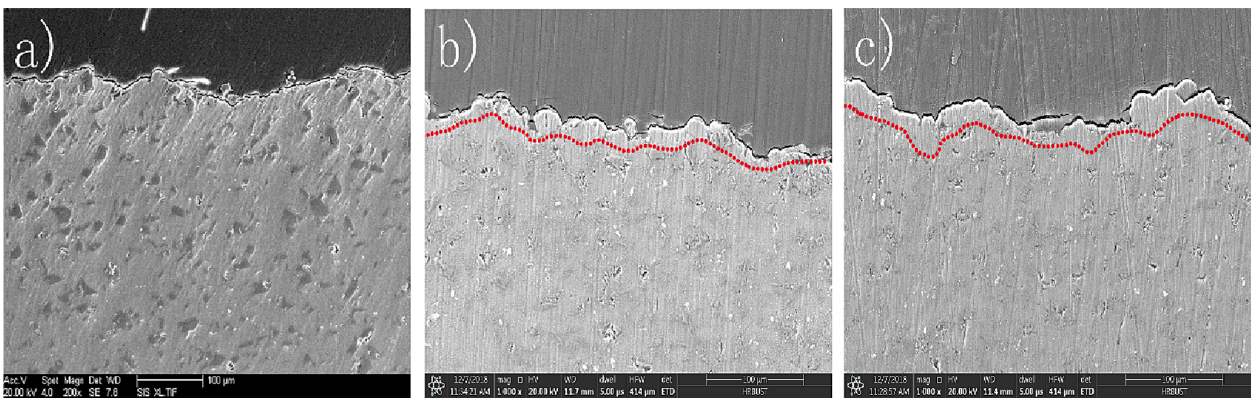

Fig. 2. Cross-section morphology of the coating after irradiation a) untreated; b) 3 J/cm^2; c) 4.5 J/cm^2.

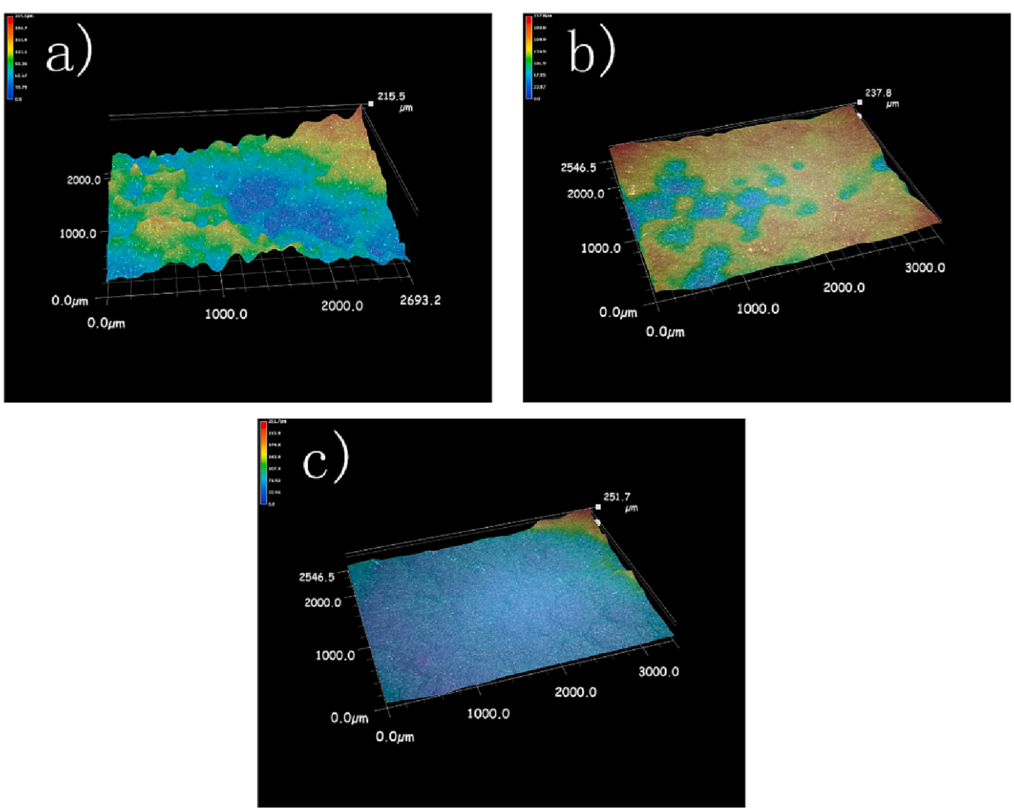

Fig. 3. Three-dimensional surface morphology of the coating treated with different energy density a) untreated; b) 3 J/cm^2; c) 4.5 J/cm^2.

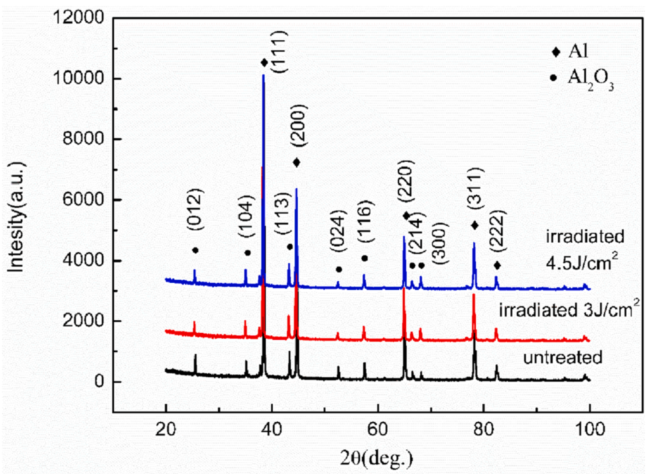

Fig. 4. XRD patterns of the untreated and treated coatings.

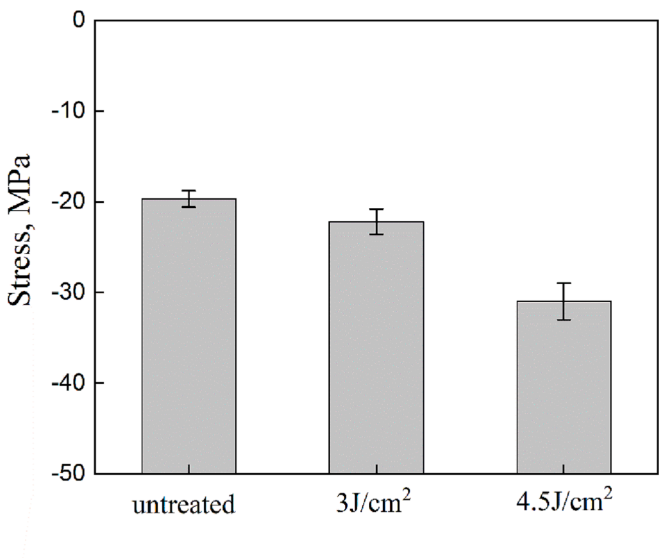

Fig. 5. Stress on the coating surface before and after irradiation.

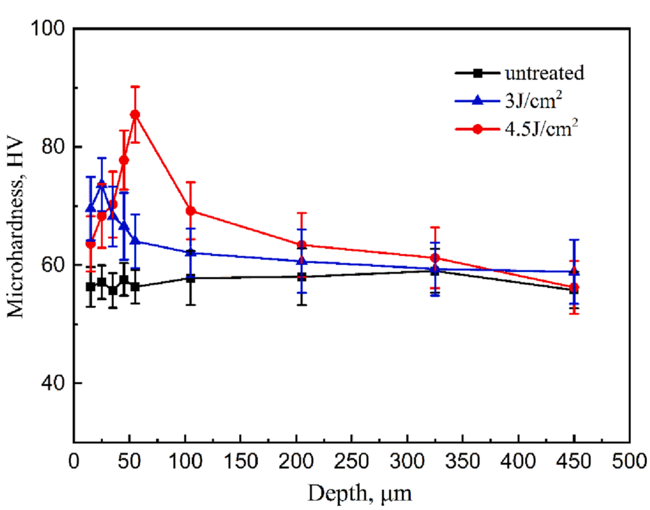

Fig. 6. Microhardness of the coating before and after irradiation.

This change in the friction coefficient is probably attributed to the rough and undulating surface of the untreated sample, while the surface of HCPEB treated samples is relatively smooth and dense. The friction coefficient of the HCPEB treated samples is lower than that of the untreated coating sample. Fig. 8 shows the widths and depths of wear tracks after the wear tests. The configurations of wear tracks were significantly different. The wear width of the untreated sample was 430 μm, and after HCPEB treatment, it decreased to 118 and 186 μm, respectively. The wear track depth decreases from 52 μm to 14 and 22 μm, respectively. The wear track width and depth of the HCPEB irradiated coating tended to decrease with increasing irradiation energy density. The remelted layer with high hardness and compressive stress enhances the sliding wear resistance of the sample. The wear resistance of the treated coating was influenced by the microhardness and residual stress of the surface and subsurface layers. The grain size in the remelted layer of the coating surface is typically refined by means of electron beam irradiation treatment, which impedes dislocation movement and enhances deformation resistance. This results in an improvement in both plastic deformation capacity and surface microhardness. As the residual compressive stress increases, the number of voids and defects on the coating surface decreases while crack propagation is inhibited. The thermo-mechanical coupling effect of a high current pulsed electron beam induces dynamic strain strengthening and improves surface quality, thereby enhancing the wear resistance of the coating.

Fig. 9 shows the corrosion resistance test results of coating samples before and after HCPEB irradiation. The corrosion current density (I_{corr}) and corrosion potential (E_{corr}) are used to evaluate the corrosion resistance of the coating, plotted in Fig. 9b. The E_{corr} value of the untreated sample was −1.12 V, and the E_{corr} value of the HCPEB treated sample was −0.98, −0.95 V, respectively. The E_{corr} value of the samples increased significantly after HCPEB irradiation, which implies that would be more difficult to corrode. The I_{corr} value of the untreated sample was 15.64 μA/cm^2, and the I_{corr} value of the HCPEB treated sample was 11.29, and 3.31 μA/cm^2, respectively, which suggests that the corrosion rate of irradiated samples was lower than that of the untreated sample during the corrosion process. As shown in Fig. 10, the Nyquist plots of the untreated and HCPEB treated Al coating samples are given. According to the theory of electrochemical impedance spectroscopy, the high frequency capacitive loop is usually attributed to the charge transfer resistance [33,34]. As shown in Fig. 10, after the HCPEB treatment with 3 and 4.5 J/cm^2, the radius of the capacitive loop in Nyquist plots of the irradiated coating increased compared with that of the untreated samples, proving that the corrosion resistance of the treated samples improved. It indicates that the irradiated coating polarization resistance was increased and the coating protective performance was improved. The surface defects of cold spraying coating like large cavities and non-molten particles can allow penetration of corrosive medium to destroy the coating, eventually, failing the protective coating. The dense surface treated by HCPEB has prevented the invasion of the corrosive medium effectively. In summary, HCPEB irradiation can improve the surface quality，wear resistance and corrosion resistance of the Al coating by cold spray.

4. Conclusions

High current pulsed electron beam was used for the irradiation of cold spray Al coating. The evolution of structure and properties of cold spray Al coating surface before and after irradiation were investigated. The main conclusions are summarized as follows:

(1) The surface of the Al coating developed a remelted layer with a thickness of about 20 μm after electron beam irradiation; this decreased the surface flaws of the cold spraying coating, such as large voids and non-molten particles, and made the coating surface dense and smooth. The surface quality of cold spray Al coatings was improved by HCPEB treatment. The Al phase as well

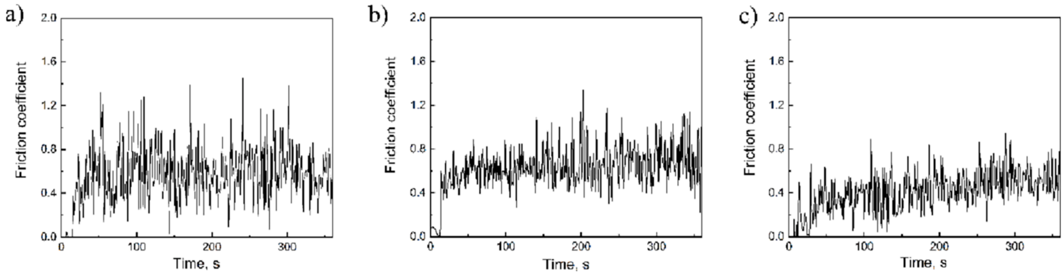

Fig. 7. Friction coefficient curves of the coatings at a) untreated, b) 3 J/cm^2 treated, and c) 4.5 J/cm^2 treated.

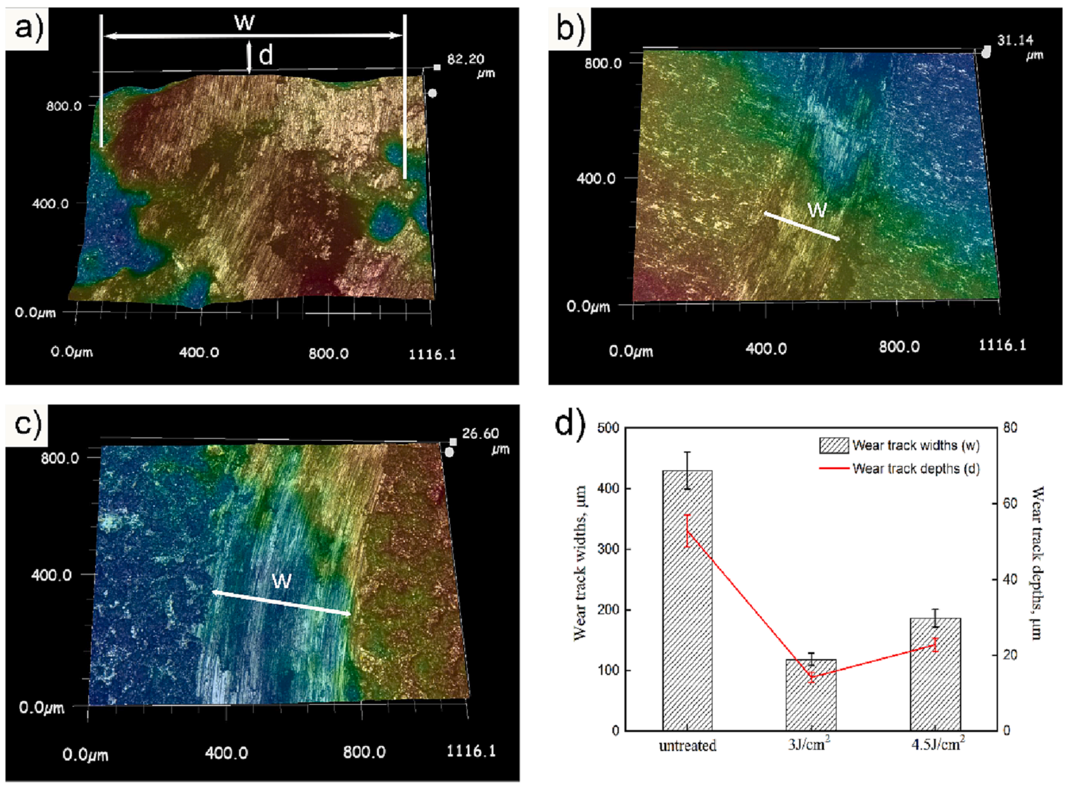

Fig. 8. Three-dimensional wear tracks morphology of the coating surface a) untreated; b) 3 J/cm^2; c) 4.5 J/cm^2; d) width and depth of wear tracks measured at (a)-(c).

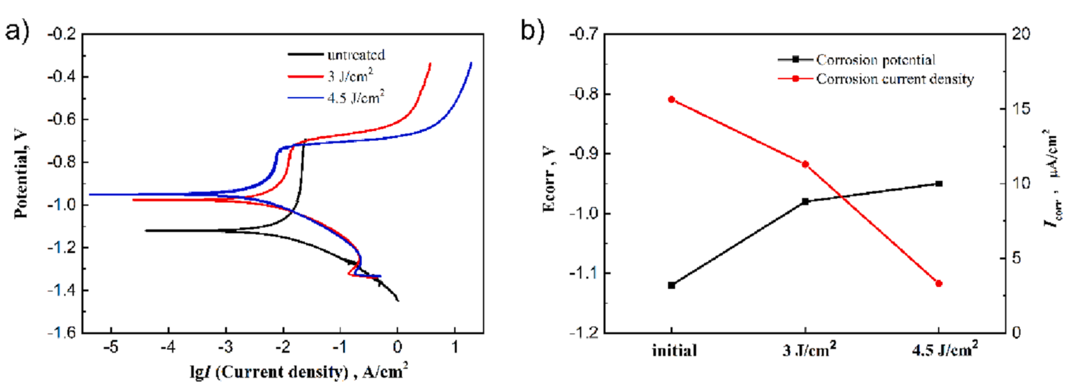

Fig. 9. (a)The polarization curves of coating samples before and after irradiation in 3.5 wt% NaCl solution, (b)Variation of corrosion current density (Icorr) and corrosion potential (Ecorr).

as the corundum phase was detected in the initial and treated coating samples.

(2) After electron beam irradiation, the compressive residual stress and microhardness of the coating surface were increased. The highest microhardness of the treated coatings occurs in the

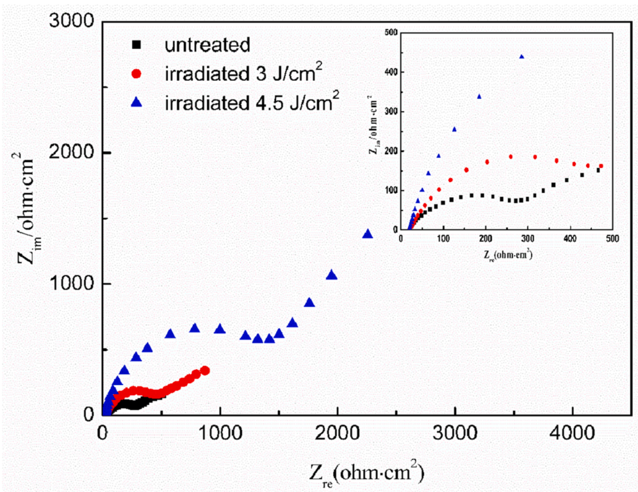

Fig. 10. Nyquist plots of the untreated and treated coating samples.

subsurface layer of the coatings. After being irradiated by HCPEB with the energy density of 3 and 4.5 J/cm^2, the wear track width and the wear track depth of the Al coating were reduced, and the wear resistance of the Al coating was significantly enhanced.

(3) The corrosion resistance of Al coating was improved by surface densification. After being irradiated by HCPEB with the energy density of 3 and 4.5 J/cm^2, the corrosion potential of the Al coating has increased from −1.12 to −0.98 and −0.95 V, respectively, and the corrosion current density has reduced from 15.64 to 11.29 and 3.31 μA/cm^2, respectively.

CRediT authorship contribution statement

Wei Jiang: Conceptualization, Methodology, Data curation, Writing – original draft, Writing – review & editing. **Yuanliang Sun:** Visualization, Data curation. **Hongbin Dai:** Methodology, Validation. **Enhao Wang:** Methodology, Writing – review & editing.

Declaration of Competing Interest

The authors declare that they have no known competing financial interests or personal relationships that could have appeared to influence the work reported in this paper.

Data availability

Data will be made available on request.

Acknowledgments

This work was supported by Heilongjiang Provincial Natural Science Foundation of China (LH2020E084), the Fundamental Research Foundation for Universities of Heilongjiang Province (LGYC2018JC035), and the National Natural Science Foundation of China (51901058).

References

[1] G.S. Wu, J.M. Ibrahim, P.K. Chu, Surface design of biodegradable magnesium alloys — a review, Surf. Coat. Technol 233 (2013) 2–12.
[2] V.V. Ramalingam, P. Ramasamy, M.D. Kovukkal, G. Myilsamy, Research and development in magnesium alloys for industrial and biomedical applications: a review, Met. Mater. Int. 26 (4) (2020) 409–430.
[3] W.J. Joost, P.E. Krajewski, Towards magnesium alloys for high-volume automotive applications, Scr. Mater. 128 (2017) 107–112.
[4] X.B. Chen, N. Birbilis, T.B. Abbott, Review of corrosion-resistant conversion coatings for magnesium and its alloys, Corrosion 67 (2011) 35001–35005.
[5] P. Nowak, M. Mosiałek, D. S. Kharitonov, J. Adamiec, A. Turowska, Effect of TIG welding and rare earth elements alloying on corrosion resistance of magnesium alloys, J. Electrochem. Soc. 167 (2020) 131504.
[6] Z.X. Ba, Q.S. Dong, J.H. Yin, J.X. Wang, B. Ma, X.B. Zhang, Z.Z. Wang, Surface properties of Mg-Gd-Zn-Zr alloy modified by Sn ion implantation, Mater. Lett 190 (2017) 90–94.
[7] Y.Q. Rao, Q. Wang, J.X. Chen, C.S. Ramachandran, Abrasion, sliding wear, corrosion, and cavitation erosion characteristics of a duplex coating formed on AZ31 Mg alloy by sequential application of cold spray and plasma electrolytic oxidation techniques, Mater. Today Commun. 26 (2021), 101978.
[8] S.K. Charu Singh, R.S. Tiwari, Development of corrosion-resistant electroplating on AZ91 Mg alloy by employing air and water-stable eutectic based ionic liquid bath, Surf. Coat. Technol. 428 (2021), 127881.
[9] Z. Y, Gao, D. Yang, C. J. Sun, L. T. Du, X. Z, Z. G. An, The corrosion resistance of Al film on AZ31 magnesium alloys by magnetron sputtering, Metals 11 (2021) 1522.
[10] C.L. Zhang, P. Lv, J. Cai, Y.W. Zhang, H. Xia, Q.F. Guan, Enhanced corrosion property of W-Al coatings fabricated on aluminum using surface alloying under high-current pulsed electron beam, J. Alloys Compd. 723 (2017) 258–265.
[11] W.J. Lee, J. Kim, H.W. Park, Improved corrosion resistance of Mg alloy AZ31B induced by selective evaporation of Mg using large pulsed electron beam irradiation, J. Mater. Sci. Technol. 35 (5) (2019) 891–901.
[12] W.H. Yao, L. Wu, J.F. Wang, B. Jiang, D.F. Zhang, M. Serdechnova, T. Shulha, C. Blawert, M.L. Zheludkevich, F.S. Pan, Micro-arc oxidation of magnesium alloys: a review, J. Mater. Sci. Technol. 118 (2022) 158–180.
[13] G.P. Abatti, A.T.N. Pires, A. Spinelli, N. Scharnagl, T.F.D. Conceição, Conversion coating on magnesium alloy sheet (AZ31) by vanillic acid treatment: preparation, characterization and corrosion behavior, J. Alloys Compd. 738 (2018) 224–232.
[14] H. Assadi, H. Kreye, F. Gärtner, T. Klassen, Cold spraying-a materials perspective, Acta Mater. 116 (2016) 382–407.
[15] B. Marzbanrad, H. Jahed, E. Toyserkani, On the evolution of substrate's residual stress during cold spray process: a parametric study, Mater. Des. 138 (2018) 90–102.
[16] M. Daroonparvar, H.R. Bakhsheshi-Rad, A. Saberi, M. Razzaghi, A.K. Kasar, S. Ramakrishna, P.L. Menezes, M. Misra, A.F. Ismail, S. Sharif, F. Berto, Surface modification of magnesium alloys using thermal and solid-state cold spray processes: challenges and latest progresses, J. Magnes. Alloy 10 (8) (2022) 2025–2061.
[17] S. Yin, M. Meyer, W. Li, H. Liao, R. Lupoi, Gas flow, particle acceleration, and heat transfer in cold spray: a review, J. Alloys Compd. 25 (5) (2016) 874–896.
[18] B. Marzbanrad, M.H. Razmpoosh, E. Toyserkani, H. Jahed, Role of heat balance on the microstructure evolution of cold spray coated AZ31B with AA7075, J. Magnes. Alloy 9 (4) (2021) 1458–1469.
[19] T.Y. Liao, A. Biesiekierski, C. C. Berndt, P. C. King, E. P. Ivanova, H. Thissen, P. Kingshott, Multifunctional cold spray coatings for biological and biomedical applications: a review, Prog. Surf. Sci. 97 (2022) 100654.
[20] S. M. Wan, X. F. Cui, Q. W. Jin, J. J. Ma, X. Wen, W. N. Su, X. R. Zhang, G. Jin, H. L. Tian, Microstructure and properties of cold sprayed aluminum bronze coating on MBLS10A-200 magnesium-lithium alloy, Mater. Chem. Phys. 281 (2022) 125832.
[21] R.P.S. Chakradhar, G. Chandra Mouli, H. Barshilia, M. Srivastava, Improved corrosion protection of magnesium alloys AZ31B and AZ91 by cold-sprayed aluminum coatings, J. Therm. Spray Tech. 30 (1-2) (2021) 371–384.
[22] W. Jiang, L. Wang, X. Wang, Studies on surface topography and mechanical properties of TiN coating irradiated by high current pulsed electron beam, Nucl. Instrum. Methods Phys. Res. Sect. B-Beam Interact. Mater. Atoms 436 (2018) 63–67.
[23] W.H. Peng, S.Z. Hao, J. Chen, W. Li, L.M. Zhao, J. Deng, Surface composite microstructure and improved mechanical property of YG10X cemented carbide induced by high current pulsed electron beam irradiation, Int. J. Refract. Met. Hard Mater 78 (2019) 233–239.
[24] F. Morini, M. Bestetti, S. Franz, A. Vicenzo, A. Markov, E. Yakovlev, Surface properties modification of magnesium alloys by low energy high current pulsed electron beam, Surf. Coat. Technol. 420 (2021), 127351.
[25] B. Gao, N. Xu, P.F. Xing, Shock wave induced nanocrystallization during the high current pulsed electron beam process and its effect on mechanical properties, Mater. Lett. 237 (2019) 180–184.
[26] W. Jiang, L. Wang, X. Wang, Design and characterization of the annular cathode high current pulsed electron beam source for circular components, Nucl. Instrum. Methods Phys. Res. Sect. B-Beam Interact. Mater. Atoms. 380 (2016) 71–75.
[27] M.H. Guo, Q.M. Wang, J. Gong, C. Sun, R.F. Huang, L.S. Wen, Oxidation and hot corrosion behavior of gradient NiCoCrAlYSiB coatings deposited by a combination of arc ion plating and magnetron sputtering techniques, Corros. Sci. 48 (9) (2006) 2750–2764.
[28] G. Shayegan, H. Mahmoudi, R. Ghelichi, J. Villafuerte, J. Wang, M. Guagliano, H. Jahed, Residual stress induced by cold spray coating of magnesium AZ31B extrusion, Mater. Des. 60 (2014) 72–84.
[29] K.Y. Luo, X. Jing, J. Sheng, G.F. Sun, Z. Yan, J.Z. Lu, Characterization and analyses on micro-hardness, residual stress and microstructure in laser cladding coating of 316L stainless steel subjected to massive LSP treatment, J. Alloys Compd. 673 (2016) 158–169.
[30] L.H. Zhang, C.T. Peng, J. Shi, Y.X. Jin, R.F. Lu, Influence of high current pulsed electron beam on microstructure and properties of NieW alloy coatings, J. Alloy. Compd. 828 (2020), 154460.
[31] Q.F. Guan, Q.Y. Zhang, C. Dong, Physical model of stress and deformation microstructures in AISI 304L austenitic stainless steel induced by high-current pulsed electron beam surface irradiation, ISIJ Int. 48 (2008) 235–239.

[32] L.X. Song, K.M. Zhang, J.X. Zou, P. Yan, Surface modifications of a hyperperitectic Zn-10 wt% Cu alloy by pulsed electron beam treatment, Surf. Coat. Technol. 388 (2020), 125530.
[33] Y.R. Liu, K.M. Zhang, J.X. Zou, D.K. Liu, T.C. Zhang, Effect of the high current pulsed electron beam treatment on the surface microstructure and corrosion resistance of a Mg-4Sm alloy, J. Alloys Compd. 741 (2018) 65–75.
[34] E. Abedi Esfahani, H. Salimijazi, M.A. Golozar, J. Mostaghimi, L. Pershin, Study of corrosion behavior of arc sprayed aluminum coating on mild steel, J. Therm. Spray Technol. 21 (6) (2012) 1195–1202.